

Magnetic properties of coordination clusters with $\{\text{Mn}_4\}$ and $\{\text{Co}_4\}$ antiferromagnetic cores.

Simona Achilli,^{*ab} Claire Besson,^c Xu He,^d
Pablo Ordejón,^d Carola Meyer^e, Zeila Zanolli^{f,b,d}

^a Dipartimento di Fisica "Aldo Pontremoli", Università degli Studi di Milano, Via Celoria 16, Milan, Italy, simona.achilli@unimi.it

^b European Theoretical Spectroscopy Facilities

^c Department of Chemistry, The George Washington University, Washington DC 20052, USA.

^d Catalan Institute of Nanoscience and Nanotechnology (ICN2), CSIC and BIST, Campus UAB.

^e Department of Physics, Universität Osnabrück, 49076 Osnabrück, Germany.

^f Chemistry Department, Debye Institute for Nanomaterials Science, Condensed Matter and Interfaces, Utrecht University, PO Box 80 000, 3508 TA Utrecht, The Netherlands.

1 Synthesis and characterization

1.1 Materials and synthesis

2-aminophenol (> 98%, TCI) was recrystallised from boiling water, washed with ice-cold water and diethylether and stored under inert atmosphere. 2,6-diacetylpyridine (> 98%, TCI), $\text{Co}(\text{OAc})_2 \cdot 4 \text{H}_2\text{O}$ (99.999% trace metal basis, Aldrich) and $\text{Zn}(\text{OAc})_2 \cdot 2 \text{H}_2\text{O}$ (99.999% trace metal basis, Aldrich) were used as received. Solvents were, when indicated, deaerated by three freeze-pump-thaw cycles using argon as inert gas. PE spatulas and PTFE cannulas were employed to avoid magnetic contamination of the samples.

$[\text{Mn}_4\text{OAc}_4\text{L}_2]$ ($\text{H}_2\text{L} = 2,6\text{-bis-(1-(2-hydroxyphenyl)iminoethyl)pyridine}$) ($\{\text{Mn}_4\}$)

The complex was synthesized according to the literature.¹

$[\text{Co}_4\text{L}_2(\text{OAc})_4]$ ($\text{H}_2\text{L} = 2,6\text{-bis-(1-(2-hydroxyphenyl)iminoethyl)pyridine}$) ($\{\text{Co}_4\}$)

Synthesis of the complex follows the preparation of the manganese analogue,¹ with some modifications. In particular, conducting the reaction under protective atmosphere is necessary to avoid the formation of an unidentified brown precipitate by the reaction of 2-aminophenol, cobalt acetate and dioxygen. 2,6-diacetylpyridine (439 mg, 2.5 mmol, 1 eq.), 2-aminophenol (583 mg, 5.3 mmol, 2.2 eq.) and $\text{Co}(\text{OAc})_2 \cdot 4 \text{H}_2\text{O}$ (1.33 g, 5.3 mmol, 2.2 eq.) were introduced in a Schlenk flask under argon. Deaerated methanol (10 mL) was cannulated into the flask and the resulting red solution was refluxed under argon for two hours. After the solution was returned to room temperature, deaerated diethylether (100 mL) was cannulated in and allowed to mix with the solution, yielding an orange microcrystalline precipitate. The solid was filtered and washed with diethylether (3×30 mL) to yield $\text{Co}_4\text{L}_2(\text{OAc})_4 \cdot 4 \text{CH}_3\text{CN}$ (1.0-1.2 g, 0.8-0.9 mmol, 60-70 %) as a dark orange powder. The compound was recrystallised by dissolving the solid (130 mg, 0.1 mmol) in acetonitrile (25 mL), sonicating and filtering solution and setting it up for gas phase diffusion of diethylether. Dark red crystals of $\text{Co}_4\text{L}_2(\text{OAc})_4 \cdot 4 \text{CH}_3\text{CN}$ (65-100 mg, 50-75 % recrystallisation yield) were collected by filtration after 3-4 days and used for all further characterization and reactions.

UV (CH_3CN) λ_{max} , nm (log ϵ): 260sh (4.50), 321 (4.27), 398 (4.14).

CV $E_{1/2}$, V vs. Fc^+/Fc : 0.30, 0.80.

TGA (N_2 , 10 $\text{K} \cdot \text{min}^{-1}$) -12.3 % (50-150 K, -4 CH_3CN (th. -12.4 %)). -30.5 % (350-400 K), -9.4 % (400-520 K).

Single crystal diffraction quality material can be obtained by gas phase diffusion of *n*-pentane into a saturated ethanol solution. The compound crystallizes in the $P4/n$ space group with ethanol as a solvate. Due to twinning of

the crystals and disorder of the solvate molecules we were only able to refined to a wR^2 of 36 %. The asymmetric unit unequivocally contains a $\text{Co}_4\text{L}_2(\text{OAc})_4$ molecule and an ethanol molecule hydrogen bound to one of the acetate oxygens, as well as a second ethanol molecule which refines satisfactorily with a two-parts disorder of the hydroxyl group with approximatively equal occupancies. The SQUEEZE routine was used to account for the residual electronic density localised in the large voids of the unit cell, which corresponds to 8 ethanol molecules per unit cell, yielding a final wR^2 of 36 % ($R_1 = 18$ %) with a formula $\text{Co}_4\text{L}_2(\text{OAc})_4 \cdot 3 \text{EtOH}$. Crystal structure data is available from Cambridge Structural Database, under CCDC number 1855019.

$\text{Zn}_4\text{L}_2(\text{OAc})_4$ ($\text{H}_2\text{L} = 2,6\text{-bis-(1-(2-hydroxyphenyl)iminoethyl) pyridine}$) ($\{\text{Zn}_4\}$)

Synthesis of the complex follows the preparation of the manganese analogue,¹ with some modifications. Specifically, 2,6-diacetylpyridine (186 mg, 1.0 mmol, 1 eq.), 2-aminophenol (250 mg, 2.3 mmol, 2.3 eq.) and $\text{Zn}(\text{OAc})_2 \cdot 2 \text{H}_2\text{O}$ (501 g, 2.3 mmol, 2.3 eq.) were introduced in a Schlenk flask under argon. Deaerated methanol (10 mL) was cannulated into the flask and the resulting yellow solution was refluxed under argon for two hours. Note that this step can be conducted in air, but in that case a small amount of strongly red-colored 2-amino-3H-phenoxazin-3-one is formed by the oxidative dimerisation of 2-aminophenol and contaminates the product obtained before recrystallisation. After the solution was returned to room temperature, a microcrystalline yellow solid was precipitated by the addition of diethylether (200 mL). The solid (590-640 mg) was filtered, washed with diethylether (4×25 mL), and redissolved in chloroform (100 mL). Pentane was allowed to diffuse in the solution from the gas phase (to accelerate the process, the solution was divided in three fractions). Yellow single crystal diffraction quality $\text{Zn}_4\text{L}_2(\text{OAc})_4 \cdot 4.5 \text{CHCl}_3$ (350-400 mg, 40-45 % yield) was collected by filtration after 3-4 days and used for all further characterization and reactions.

The compound crystallised in the $\text{P2}_1/\text{n}$ space group, with 4.5 CHCl_3 molecules and a $\text{Zn}_4\text{L}_2(\text{OAc})_4$ complex in the asymmetric unit. One of the chloroform molecules is located close to the inversion center at (0, 0.5, 0) and has an occupancy of 0.5. Another could be refined as an approximately 1:1 disorder between two close positions. Residual electronic density lies mostly in close proximity with the chlorine atoms of the other chloroform molecules, but attempts at refining similar disorder yielded only small occupancy factors and no significant improvement of the R factors, and were abandoned, leaving a final wR^2 factor of 12 % ($R_1 = 4.3\%$). Crystal structure data is available from Cambridge Structural Database, under CCDC number 1855020.

UV (CH_3CN) λ_{max} , nm ($\log \epsilon$): 265sh (4.40), 293 (4.23), 346 (4.17), 407 (4.23).

SQUID: χ_{dia} , $\text{m}^3 \cdot \text{mol}^{-1}$ ($\text{emu} \cdot \text{mol}^{-1}$): -5.3×10^{-9} (4.2×10^{-4}).

2 Fit of SQUID data

The experimental magnetic susceptibility was fitted exploiting an Heisenberg model Hamiltonian in which the exchange coupling parameters between pairs of ions are left as free parameters. The fit functions are reported in Figure 1 as solid lines, together with the experimental data (points) and the J_n extracted from the fit.

The J_n obtained are in fair agreement with those extracted from the LDA+U calculation. The fitted g-factor is ~ 2 in $\{\text{Mn}_4\}$ confirming the validity of the spin-only approximation, while it deviates from 2 in $\{\text{Co}_4\}$ reflecting the role of SOC.

Through the model Hamiltonian with parameters obtained from the fit of the experimental data the magnetization was calculated at different temperatures and fields. For large fields or large temperatures the magnetization of $\{\text{Mn}_4\}$ is larger than that of $\{\text{Co}_4\}$, as observed in the experiments. The saturation value ($gS\mu_B$) of $\{\text{Mn}_4\}$ ($20\mu_B$) is indeed larger than for $\{\text{Co}_4\}$ ($12\mu_B$ in a spin-only model). At low temperature, fields of 20 T for $\{\text{Co}_4\}$ and 25 T for of $\{\text{Mn}_4\}$ are needed for the magnetization to reach saturation. These values are significantly large compared to the fields accessible in our experiments (Fig. 3 in the main text).

In the low field–low-temperature limit the model shows an inversion of the magnetization curves leading to larger magnetization of $\{\text{Co}_4\}$ with respect to $\{\text{Mn}_4\}$. Moreover the two curves display opposite curvature, in agreement with SQUID data at low temperature. In particular, the magnetization of $\{\text{Mn}_4\}$ shows positive curvature, as expected for an antiferromagnet, while for $\{\text{Co}_4\}$ an almost linear dependence on the field can be observed.

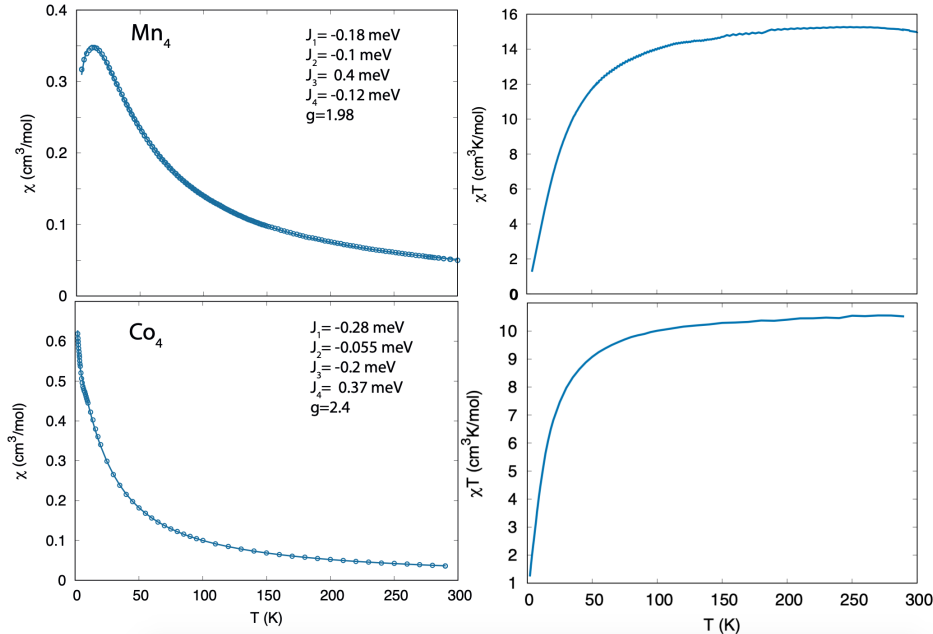


Figure 1: Left panels: Experimental (dots) magnetic susceptibility (χ cm³/mol) of $\{\text{Mn}_4\}$ and $\{\text{Co}_4\}$ with the relative fit (line). The J derived from fitting are reported as inset together with the value of g . Right panels: experimental susceptibility times temperature ($\chi \times T$, cm³K/mol) of $\{\text{Mn}_4\}$ and $\{\text{Co}_4\}$ as a function of the temperature.

The slope of the magnetization is an indication of the coupling between the magnetic centers: the stronger the antiferromagnetic coupling, the smaller the slope. Moreover, the smaller the moment per atom, the stronger the linear dependence of M on the field. Both these aspects explain the fast rise observed for the magnetization of $\{\text{Co}_4\}$ in the experimental data, as due to the smaller value of S (or J) (see table 4 and 5 in the main text) and of the AFM coupling, with respect to $\{\text{Mn}_4\}$. On the other hand, the saturation value for the magnetization of $\{\text{Co}_4\}$ is smaller than for $\{\text{Mn}_4\}$, thus the two magnetization curves show a crossing for a certain value of the field which is not reached in the experiments. At high temperature the magnetization curves flatten, resulting in a slower growth as a function of the field with respect to the low temperature limit. The linear dependence on the field $M = Ng^2S(S+1)\mu_B^2B$ in this case is governed by the value of S and it is smaller for $\{\text{Co}_4\}$ than for $\{\text{Mn}_4\}$, in agreement with what observed in the experiments at high temperature.

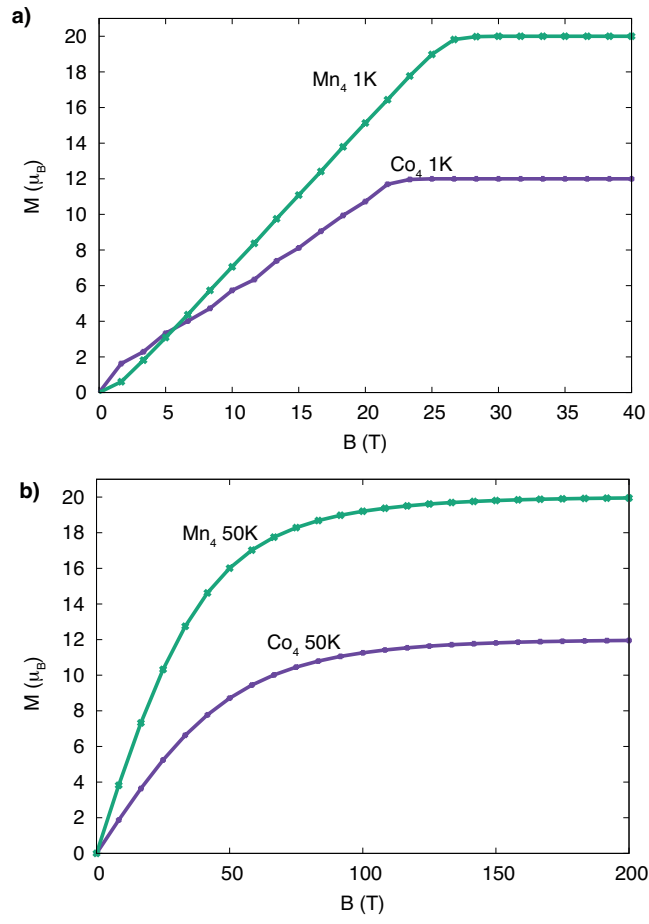


Figure 2: Magnetization versus field dependence for $\{Mn_4\}$ and $\{Co_4\}$ at 1 K (a) and 50 K (b).

3 Exchange parameters from different calculations

The exchange parameters were extracted by fitting a system of equations for the five lowest energy spin configurations of the molecule, as reported in the main text. For a comparison with the available experimental data and previous theoretical calculations on $\{\text{Mn}_4\}$ we considered also a set of only three J parameters, despite the oversimplification of this model. Indeed the assumption $J_3 = J_{(1,2)} = J_{(3,4)}$ is not correct, as the M_1/M_2 and M_3/M_4 pairs are not equivalent in terms of chemical coordination and ligands groups. The obtained values are reported in Table 1. For a system of three exchange parameters, we recover the experimental results of Kampert *et al.*¹.

In Table 2 the J parameters obtained in LDA+SOC calculation are reported. Notably, they are too large compared to those extracted from LDA+U calculation and from the experiments, confirming the need to include the electronic correlation for a reliable estimate of the exchange interaction.

In addition, we also computed the J values with the Liechtenstein-Katsnelson-Antropov-Gubanov (LKAG) formula² implemented in the TB2J package.³

Table 1: Computed exchange parameters J (meV and Kelvin) for the $\{\text{Mn}_4\}$ molecular complex, using LDA+U and a three- J Heisenberg model. The experimental values from Ref.¹ are reported for comparison.

J	J_1 (1-4,2-3)	J_2 (1-3,2-4)	J_3 (1-2, 3-4)
$\{\text{Mn}_4\}$ (meV)	-0.7	-0.4	-0.2
$\{\text{Mn}_4\}$ (Kelvin)	-8.1	-4.1	-2.0
Exp ¹ (Kelvin)	-2.2	-1.1	-0.1

Table 2: Exchange coupling parameters (J_i , meV) of $\{\text{Mn}_4\}$ and $\{\text{Co}_4\}$ molecular complexes extracted from DFT calculations with SOC included. S is normalized to 1.

SOC (meV)	J_1	J_2	J_3	J_4
$\{\text{Mn}_4\}$	-5.0	-4.2	9.3	31.8
$\{\text{Co}_4\}$	-7.35	-1.42	2.58	5.52

TB2J evaluates the J for each couple of atoms. So there are six J parameters (Table 3). The non-equivalent J for pairs M_1/M_3 and M_2/M_4 is related to the not perfect symmetry of the electronic structure associated with these pairs of atoms, probably due to some orbital polarization in the Mn/Co.

When the Heisenberg equation is solved for four exchange parameters, The TB2J results for the LDA+U case give the same trend obtained using SIESTA total energies: the ferromagnetic coupling between atoms M_1 and M_2 is not reproduced ($J_3 < 0$) and the exchange coupling parameters are larger for $\{\text{Co}_4\}$ than for $\{\text{Mn}_4\}$.

With SOC included, the exchange parameters obtained with TB2J are in fair agreement with those reported in the main text supporting the robustness of the results. The comparison between the two molecules confirms indeed the larger strength of the magnetic coupling in $\{\text{Mn}_4\}$ with respect to $\{\text{Co}_4\}$ but the absolute value of the J is too large.

All the methods agree in the qualitative description of the magnetic coupling within the two molecules and in these terms, i.e. only qualitatively, these parameters should be taken into account.

Table 3: J of the $\{\text{Mn}_4\}$ and $\{\text{Co}_4\}$ molecular complexes obtained with TB2J in LDA+U and with SOC included. The values are reported in meV.

LDA+U	J_1 (1-4,2-3)	J_2 (1-3,2-4)	J_3 (1-2)	J_4 (3-4)
$\{\text{Mn}_4\}$	-1.21/-1.23	-1.77/-1.84	-0.8	0.1
$\{\text{Co}_4\}$	-3.47/-3.29	-1.70/-1.82	0.03	-2.25
SOC	J_1 (1-4,2-3)	J_2 (1-3,2-4)	J_3 (1-2)	J_4 (3-4)
$\{\text{Mn}_4\}$	-34.5/1.3	-55.7/-29.2	12.94	3.29
$\{\text{Co}_4\}$	-3.24/-5.09	-11.84/-10.68	1.18	18.35

4 Spin dynamics calculation

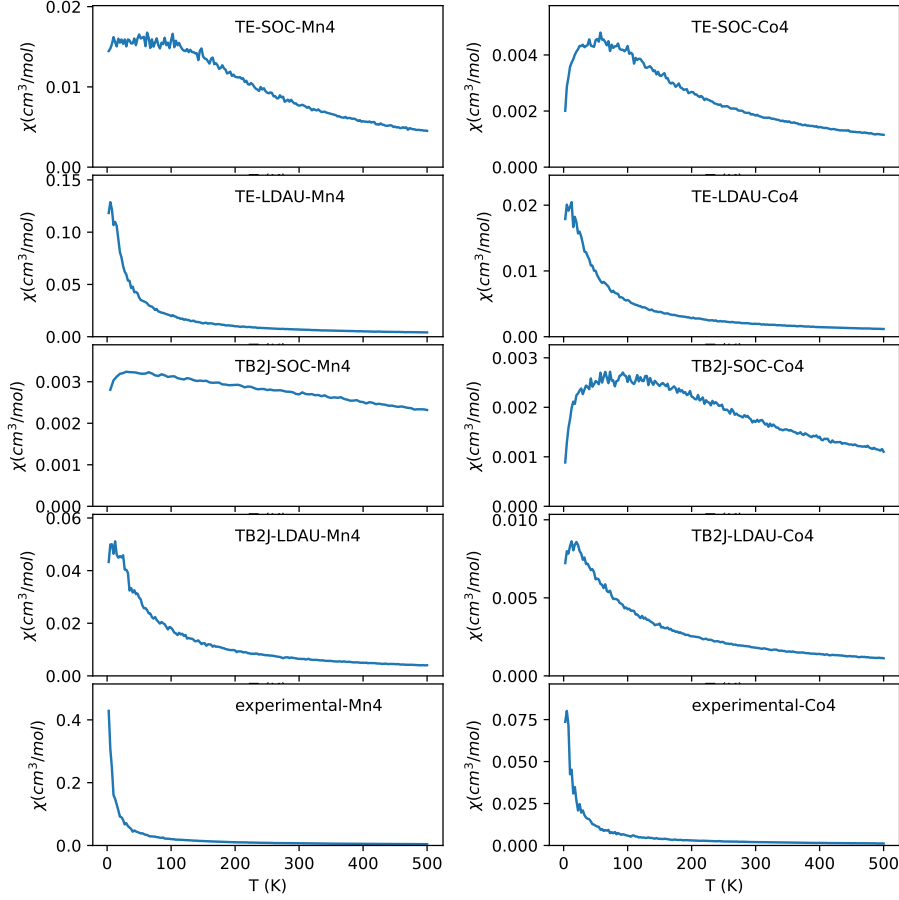


Figure 3: The susceptibilities computed with spin dynamics using various set of parameters. TE-SOC: fit from DFT (with SOC) energies. TE-LDAU: fit from DFT (with +U correction). TB2J-SOC: computed with TB2J from DFT with SOC. TB2J-LDAU: computed from TB2J with DFT+U. Experimental: fit from experimental data. The left and the right panels are from Mn4 and Co4, respectively.

Using the Heisenberg model constructed from DFT results, we perform Ginzberg-Landau-Lifshitz (GLL) atomic spin dynamics^{4,5} (ASD) to compute the magnetic susceptibility with the MULTIBINIT code⁶. The isothermal magnetic susceptibility is calculated with the fluctuation-dissipation theorem⁷:

$$\chi = \frac{1}{k_B T} (\langle m^2 \rangle - \langle m \rangle^2), \quad (1)$$

where $\langle \rangle$ means the average over the ensembles, m is the magnetization of the system.

Four sets of parameters from DFT results with either SOC or Hubbard U correction, computed by total energy (TE) method or TB2J, were used as input. Another set of exchange parameters by fitting to experimental data is also taken as comparison. The results are shown in Fig. 3.

The "λ"-shape of the susceptibility curves are similar to extended structures, where the susceptibility diverges at the critical temperature, which is ill-defined in molecules. Nevertheless the temperature of the peak (defined as T_P), the decay of the susceptibility above the T_P , and the value of the susceptibilities, all shows that the exchange parameters from the DFT results with the "+U" correction agrees better with experiments, in which the exchange values are smaller in general.

5 Relaxed structures

The atomic coordinates (in Å) obtained through structural relaxation performed in DFT-LDA and SOC included are reported below for {Co₄} and {Mn₄}.

{Co₄}:

Co 11.784660 24.970504 9.657395
Co 10.497270 22.083542 10.349018
Co 13.826910 22.493219 9.595356
Co 11.640250 22.424358 7.355454
O 12.276659 23.190641 10.768667
O 13.053111 23.738692 8.233238
O 12.150853 21.350956 8.965670
O 10.536075 23.509294 8.730816
N 11.150917 25.250576 11.697139
N 10.234291 26.256309 9.631992
N 11.898964 25.955696 7.819901
C 12.573409 23.459183 12.047217
C 13.501743 22.727320 12.800231
H 14.089320 21.934242 12.292846
C 13.683728 23.040467 14.147378
H 14.424537 22.471937 14.743995
C 12.967844 24.084895 14.745447
H 13.125847 24.329670 15.812985
C 12.094520 24.862400 13.986050
H 11.619728 25.748710 14.442161
C 11.894341 24.565336 12.624100
C 10.126773 26.025442 11.948916
C 9.578037 26.345785 13.287772
H 10.175627 27.151091 13.781884
H 8.530036 26.715922 13.221056
H 9.604646 25.444738 13.951800
C 9.538585 26.565027 10.740648
C 8.341386 27.295098 10.668957
H 7.820799 27.608225 11.593808
C 7.833021 27.630308 9.415343
H 6.862677 28.154484 9.327204
C 8.583412 27.341326 8.274367
H 8.239272 27.639455 7.265994
C 9.816490 26.700082 8.429924
C 10.790725 26.483101 7.373647
C 10.499096 26.837914 5.965518
H 11.118355 26.205940 5.283527
H 9.420716 26.654751 5.742013
H 10.706556 27.914849 5.751836
C 13.024326 25.741449 7.058258
C 13.537168 26.594422 6.071137
H 13.031246 27.555676 5.858676
C 14.722039 26.250453 5.422129
H 15.143996 26.930256 4.657679
C 15.384636 25.058139 5.746152
H 16.319763 24.794952 5.214912
C 14.880653 24.193928 6.719788
H 15.372314 23.234492 6.981271
C 13.696788 24.537235 7.377188
N 11.408346 20.414618 11.203267
N 10.045893 22.163800 12.313801

N 8.804952 23.397905 10.567973
C 12.292475 20.027330 9.077568
C 12.842500 19.207261 8.088787
H 13.105214 19.659644 7.110727
C 13.063406 17.859247 8.376878
H 13.502886 17.200660 7.602911
C 12.747203 17.325275 9.633942
H 12.915108 16.251224 9.840454
C 12.205322 18.140545 10.625957
H 11.907104 17.720989 11.605658
C 11.969344 19.493931 10.348564
C 11.650265 20.474168 12.485497
C 12.636444 19.653283 13.225367
H 13.450079 19.328860 12.531885
H 13.088399 20.253265 14.051051
H 12.169384 18.748781 13.685771
C 10.832454 21.468847 13.158681
C 10.796516 21.686320 14.539889
H 11.495754 21.142632 15.202811
C 9.837013 22.560233 15.053198
H 9.769746 22.736793 16.143428
C 8.934736 23.169554 14.182981
H 8.097913 23.779891 14.572506
C 9.094103 22.979726 12.800664
C 8.331740 23.643350 11.763572
C 7.163003 24.495043 12.088568
H 6.207428 23.931855 11.948397
H 7.186354 24.831516 13.149891
H 7.130370 25.394655 11.423137
C 8.324216 23.904560 9.387352
C 7.023869 24.354608 9.088815
H 6.233333 24.332011 9.859428
C 6.706528 24.748870 7.789651
H 5.679835 25.092977 7.561875
C 7.661627 24.652798 6.770087
H 7.379020 24.906744 5.729114
C 8.956450 24.210011 7.041607
H 9.719280 24.084856 6.245056
C 9.303374 23.877674 8.358257
O 13.550916 25.687501 10.333671
O 14.950837 23.896252 10.435570
C 14.509448 25.023697 10.844952
C 15.140291 25.589838 12.078773
H 16.108362 25.094580 12.300594
H 15.260569 26.691401 11.992143
H 14.438239 25.391374 12.931510
O 9.264080 21.016327 9.158996
O 9.981759 21.377015 7.029957
C 9.077203 21.170511 7.908653
C 7.656352 21.159999 7.435931
H 7.600703 21.151344 6.327734
H 7.105154 20.298050 7.871949
H 7.167930 22.096305 7.813696
O 14.512862 20.887840 10.767680
O 15.138232 21.186628 8.688865
C 15.122061 20.452460 9.730707

C 15.736798 19.099933 9.768206
H 16.570752 19.090335 10.507721
H 14.961592 18.371446 10.113626
H 16.110875 18.800866 8.767205
O 12.909671 21.999680 5.790142
O 11.488189 23.663316 5.667504
C 12.484160 23.030674 5.173137
C 13.128020 23.549145 3.938469
H 14.056502 22.988709 3.703249
H 12.409620 23.476724 3.089349
H 13.369196 24.629938 4.096111

{Mn₄}

Mn 11.810113 24.985996 9.743006
Mn 10.424819 22.105112 10.320622
Mn 13.969259 22.519930 9.574551
Mn 11.607671 22.312376 7.271543
O 12.349963 23.147982 10.831958
O 13.140464 23.571435 8.098263
O 12.345050 21.326161 8.840598
O 10.496148 23.528278 8.643963
N 11.103152 25.197501 11.777895
N 10.216281 26.274131 9.676366
N 11.890695 25.881198 7.790930
C 12.598813 23.438037 12.113694
C 13.538059 22.730289 12.880143
H 14.135978 21.938064 12.381465
C 13.716597 23.053512 14.225799
H 14.466366 22.503544 14.828710
C 12.981132 24.093676 14.810091
H 13.138994 24.358651 15.873515
C 12.083104 24.839617 14.047557
H 11.583453 25.716735 14.497662
C 11.870084 24.527046 12.689523
C 10.080681 25.994708 12.005918
C 9.546066 26.368410 13.338673
H 10.158648 27.184771 13.798833
H 8.501386 26.750637 13.269521
H 9.564052 25.494243 14.036190
C 9.519736 26.565525 10.790827
C 8.322393 27.297096 10.700291
H 7.771295 27.596526 11.612739
C 7.835847 27.640072 9.438633
H 6.864361 28.162054 9.339557
C 8.588967 27.345740 8.297761
H 8.238350 27.636652 7.288881
C 9.816809 26.695904 8.461386
C 10.779240 26.441424 7.388195
C 10.469343 26.827821 5.989159
H 11.084954 26.222238 5.280743
H 9.388972 26.652695 5.766540
H 10.676751 27.911245 5.802432
C 13.005089 25.665510 7.012250
C 13.513339 26.561176 6.054061
H 12.985913 27.517018 5.868582
C 14.713268 26.281899 5.401472

H 15.114912 27.003092 4.663350
C 15.418169 25.105071 5.685767
H 16.370640 24.891407 5.162735
C 14.920698 24.193405 6.616684
H 15.436848 23.237961 6.848087
C 13.721749 24.467567 7.279225
N 11.478065 20.440099 11.180512
N 10.003855 22.178942 12.333361
N 8.775266 23.494498 10.565036
C 12.408593 19.997141 9.045486
C 12.918357 19.125851 8.079778
H 13.195354 19.548705 7.091340
C 13.081014 17.774955 8.386179
H 13.483453 17.082870 7.621038
C 12.750828 17.293427 9.659596
H 12.879629 16.219411 9.896550
C 12.245944 18.156490 10.630929
H 11.933575 17.765155 11.618521
C 12.055948 19.518712 10.336676
C 11.666559 20.505982 12.473250
C 12.631942 19.682775 13.243120
H 13.452680 19.331991 12.571416
H 13.078346 20.279745 14.074642
H 12.142121 18.787278 13.701064
C 10.810985 21.480729 13.153574
C 10.777720 21.687779 14.537103
H 11.483502 21.153446 15.201722
C 9.816902 22.561530 15.054735
H 9.761617 22.737795 16.146542
C 8.914799 23.190749 14.196371
H 8.101547 23.821929 14.604057
C 9.058508 23.008922 12.809644
C 8.310229 23.711196 11.775950
C 7.116812 24.523390 12.119889
H 6.177053 23.930361 11.983475
H 7.137163 24.854052 13.184148
H 7.048056 25.426713 11.463985
C 8.294030 23.971264 9.377957
C 6.985741 24.402518 9.078548
H 6.208726 24.395808 9.864623
C 6.645107 24.768102 7.776819
H 5.611433 25.100776 7.560535
C 7.584354 24.666278 6.741623
H 7.286273 24.909318 5.702311
C 8.882809 24.228377 7.004842
H 9.636329 24.102363 6.198341
C 9.255876 23.909629 8.319972
O 13.629165 25.693699 10.335326
O 15.054352 23.949492 10.419150
C 14.579768 25.047346 10.878908
C 15.148944 25.577028 12.154026
H 16.102522 25.070021 12.411438
H 15.283882 26.679496 12.085672
H 14.405273 25.377946 12.971604
O 9.240174 20.965235 9.109180
O 9.939535 21.279195 6.990173

C 9.017738 21.132906 7.868470
C 7.596402 21.202296 7.413526
H 7.528188 21.226430 6.305692
H 7.019675 20.346110 7.830899
H 7.143116 22.142987 7.825555
O 14.587882 20.910049 10.688605
O 15.351206 21.082424 8.631351
C 15.226349 20.400428 9.687313
C 15.757963 19.019043 9.815996
H 16.581455 19.010146 10.568026
H 14.940826 18.348605 10.182828
H 16.133811 18.655074 8.836485
O 12.967978 21.908972 5.586999
O 11.521639 23.566847 5.647444
C 12.523106 22.978168 5.081699
C 13.126088 23.607245 3.878303
H 14.073814 23.096458 3.606186
H 12.402614 23.547213 3.031790
H 13.323867 24.686749 4.095232

Notes and references

- [1] E. Kampert, F. F. B. J. Janssen, D. W. Boukhvalov, J. C. Russcher, J. M. M. Smits, R. de Gelder, B. de Bruin, P. C. M. Christianen, U. Zeitler, M. I. Katsnelson, J. C. Maan and A. E. Rowan, Inorg. Chem., 2009, **48**, 11903–11908.
- [2] A. I. Liechtenstein, M. I. Katsnelson, V. P. Antropov and V. A. Gubanov, Journal of Magnetism and Magnetic Materials, 1987, **67**, 65–74.
- [3] X. He, N. Helbig, M. J. Verstraete and E. Bousquet, Computer Physics Communications, 2021, **264**, 107938.
- [4] L. Landau and E. Lifshitz, Perspectives in Theoretical Physics, Elsevier, 1992, pp. 51–65.
- [5] T. L. Gilbert, IEEE transactions on magnetics, 2004, **40**, 3443–3449.
- [6] X. Gonze, B. Amadon, G. Antonius, F. Arnardi, L. Baguet, J.-M. Beuken, J. Bieder, F. Bottin, J. Bouchet, E. Bousquet et al., Computer Physics Communications, 2020, **248**, 107042.
- [7] D. Landau and K. Binder, A guide to Monte Carlo simulations in statistical physics, Cambridge university press, 2021.